

PAPER • OPEN ACCESS

Methods for assessing the impact of the energy fields of experimental prototypes of contactless charging of implants' power supply sources on biological objects

To cite this article: A V Rabin and A A Petrushevskaya 2019 *IOP Conf. Ser.: Earth Environ. Sci.* **315** 032030

View the [article online](#) for updates and enhancements.

Methods for assessing the impact of the energy fields of experimental prototypes of contactless charging of implants' power supply sources on biological objects

A V Rabin and A A Petrushevskaya

Saint-Petersburg State University of Aerospace Instrumentation (SUAI), ul. Bolshaya Morskaya, 67, lit. A, St. Petersburg, 190000, Russia

E-mail: alexey.rabin@guap.ru, aap@guap.ru

Abstract. Currently existing bioimplants need to be periodically removed from a body to replace a source of energy supply and then reinstall them in a body. It is to a certain degree a threat to the health of the patient and degrades the quality of his life. Developed by the authors contactless charger for transcutaneous energy supply of implantable modules automatically adjusts the power of the electromagnetic field. When implementing the methodology for assessing the impact of the energy fields of experimental prototype of implant power supplies' contactless charging on biological objects, it was decided to link the transmitting and receiving modules to negative feedback loop, which allows stabilizing the power supplied to the transmitting circuit by the D class amplifier. This solution minimizes the heating of the receiving module, both in the area of the receiving circuit, and in the area of the stabilizer of the charging current of the battery. Thus, in addition to smaller dimensions, the new solution allows optimizing the energy characteristics of the device as a whole.

1. Introduction

One of the tasks of the future medicine are a creation and an implementation of the personalized medicine in practice, the basis of which will be an individual approach for each patient, including prevention, diagnosis and continuous monitoring of the health status.

Taking into account the constant growth of the percentage of the older (over 60 y.o.) population, the issue of the people's health status monitoring, including the remote one, becomes more than urgent. An important role in the implementation of such monitoring is played by the deployment of telemedicine technologies, which, according to the Federal Law No. 242-FL dated on July 29th, 2017 [1], becomes one of the priority directions of Russian medicine development. In this process implantable devices providing remote diagnostics have an important contribution.

The interest in the researchers' environment in the development and use of biotelemetric systems for remote health monitoring is related to the fact that, due to their miniaturization while expanding functional qualities, practical medicine receives new technologies.

However, in practice, the implementation of remote monitoring of livelihoods faces several problems. Implantable devices are introduced into a human body surgically, and they autonomously monitor the functioning of individual organs and systems. The currently existing bioimplants need to be periodically removed from a body to replace a source of energy supply and then reinstall them in a body.



To a certain extent, this poses a threat to the patient’s health and impairs his quality of life. It is to a certain degree a threat to the health of the patient and degrades the quality of his life [2, 3].

Thereby, the priority task is the development of a contactless charging device for a percutaneous energy supply of implantable modules, as well as the development of a methodology for assessing the impact of the energy fields of experimental prototypes on biological objects. When solving this urgent task, it is necessary to ensure high efficiency wireless energy transfer, regardless of the implant location in the patient’s body [4].

2. Integration of the contactless charging device and the implantable biotelemetric system

The experimental prototype of the contactless charging device of implants’ power supply sources consist of the receiving and transmitting modules and is shown in figure 1 and figure 2, respectively.

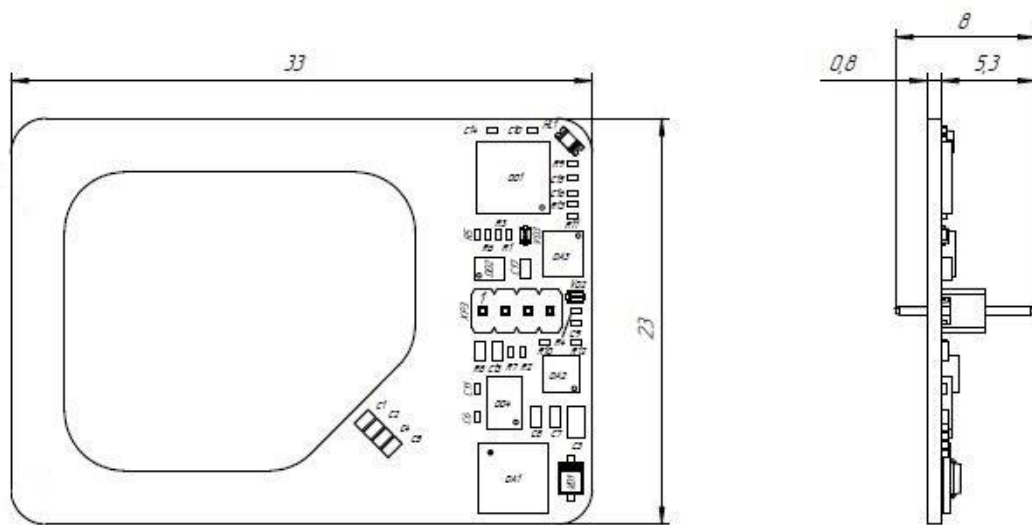


Figure 1. General drawing of the contactless charging device. Receiving module.

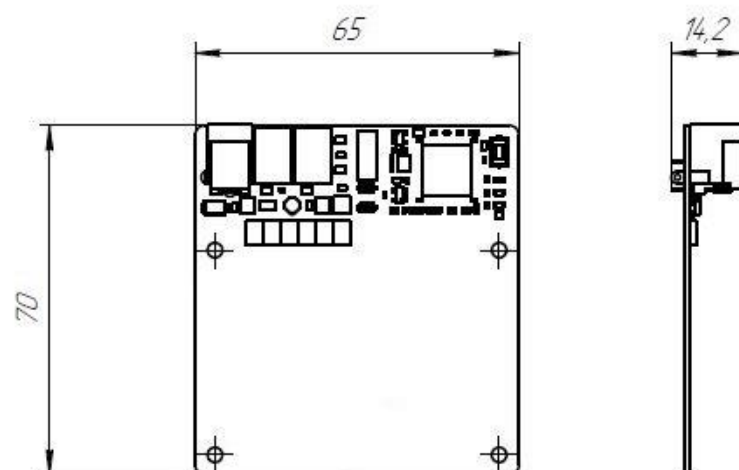


Figure 2. General drawing of the contactless charging device. Transmitting module.

The developed modules of the contactless charging device should be used in conjunction with an implantable biotelemetric system in order to assess the impact of wireless energy transfer method based on electromagnetic induction on a biological object.

The experimental prototype of the implantable biotelemetric system also consist of the receiving and transmitting modules and is shown in figures 3 and 4, respectively.

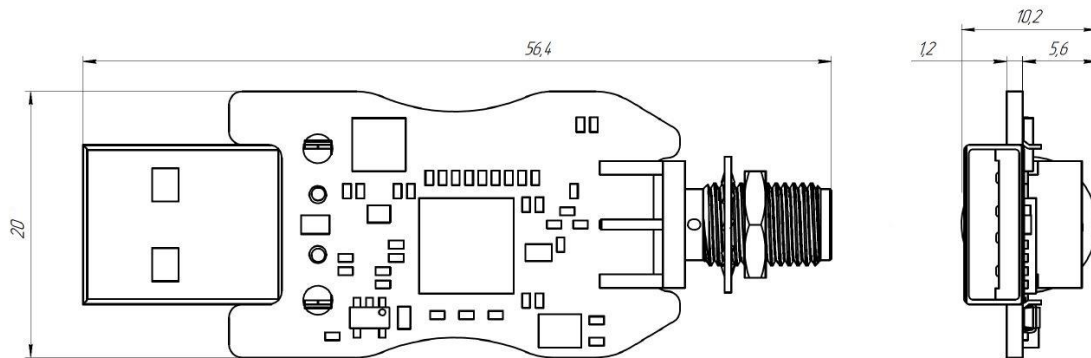


Figure 3. General drawing of the implantable biotelemetric system. Receiving module.

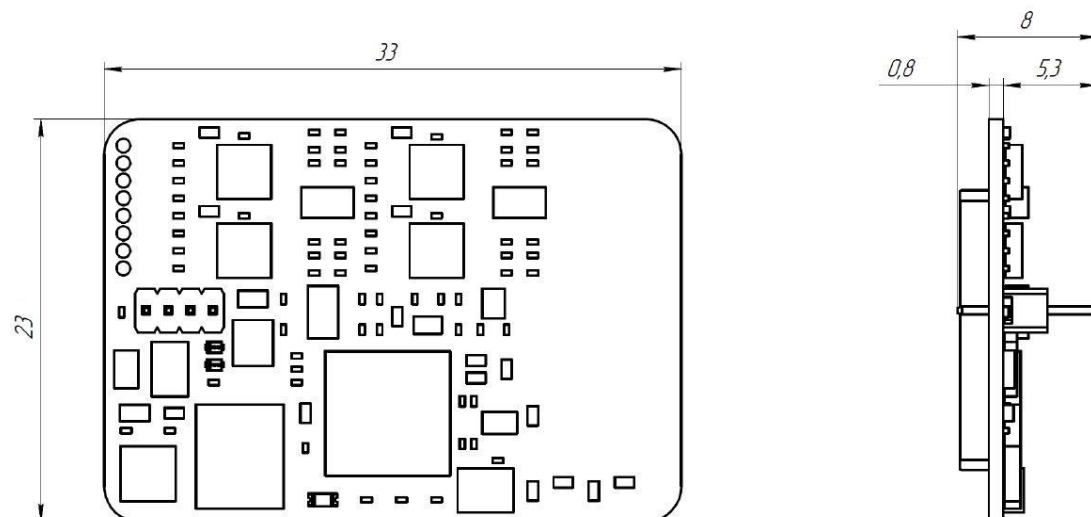


Figure 4. General drawing of the implantable biotelemetric system. Transmitting module.

The receiving module of the charging device through the board-to-board connector is connected to the transmitting module of the biotelemetric system, which, when encapsulated, can be placed inside a biological object. Charging device's transmitting module is placed on the body of a biological object opposite the charging device's receiving module and generates an electromagnetic field, the energy of which is converted at the last to charge a rechargeable power source (battery, supercapacitor) of the biotelemetry transmitting module.

3. Analytical description of assessing of the impact of the energy fields on biological objects

For correct operation of contactless charging of experimental prototypes of implant power supply sources and prevention of excessive influence of energy fields on biological objects, magnetic constant and inductance indicators were estimated by analytically calculating the value of the output current when the battery was charged.

To do this, it was necessary to calculate the inductance of both circuits first. The inductance of one turn, taking into account the winding radius r and the conductor diameter d when the condition $d/(2r) \ll 1$ is fulfilled, is calculated by the formula:

$$L(r, d) = \mu_0 r \left(\ln \left(\frac{4r}{d} \right) - 2 \right), \tag{1}$$

where $\mu_0 = 4\pi \cdot 10^{-7}$ H/m is the magnetic constant.

The mutual inductance of two round turns lying in parallel planes is described by the formula:

$$M(r_1, r_2, \rho, \delta) = \pi \mu_0 \sqrt{r_1 r_2} \int_0^\infty J_1 \left(x \sqrt{\frac{r_1}{r_2}} \right) \cdot J_1 \left(x \sqrt{\frac{r_2}{r_1}} \right) \cdot J_0 \left(x \frac{\rho}{\sqrt{r_1 r_2}} \right) \cdot e^{-x \frac{\delta}{\sqrt{r_1 r_2}}} dx, \tag{2}$$

where ρ is the axial displacement between turns, s is the distance between the planes of the turns, J_0 and J_1 are the Bessel functions of the first kind.

The total inductance of two co-wound coils is defined as

$$L = L_1 + L_2 + M_{12} + M_{21}. \tag{3}$$

Then, according to the notation adopted in figure 5, and using formulas (1)-(3), the inductance L_c of a volume multi-turn cylindrical coil can be expressed:

$$L_c = N_l \sum_{i=1}^{N_w} L_i(r_i, d) + \sum_{n=1}^{N_l} \sum_{m=1}^{N_l} \sum_{i=1}^{N_w} \sum_{j=1}^{N_w} M(r_{n,i}, r_{m,j}, 0, s \cdot |n - m|) \cdot a_{n,m,i,j}, \tag{4}$$

where N_l is the number of layers in a plane, N_w is the number of turns in the layer, $a = 0$, if $n = m$ and $i = j$, and $a = 1$, otherwise.

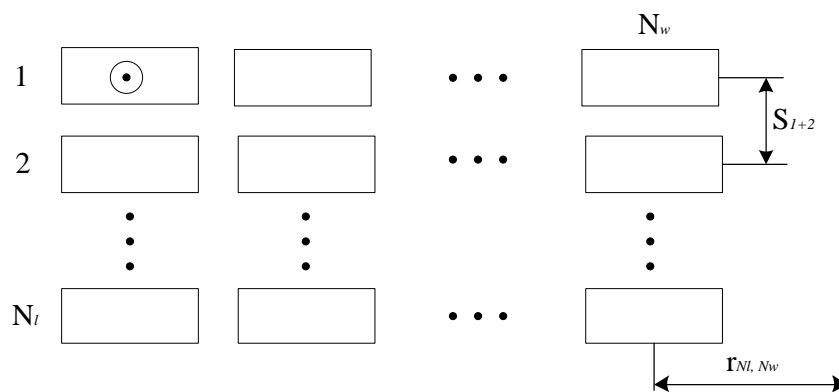


Figure 5. Geometric parameters of inductors made on the printed circuit board.

The inductance of a rectangular coil with rounded corners was determined by the formula (4) by introducing the parameter of equivalent radius r_{eq} of a cylindrical coil. The approximating function for calculating r_{eq} was chosen empirically. The boundary values of r_{eq} were determined by calculating the inductance over an equivalent area and perimeter of a rectangular coil, namely, r_{eqL} and r_{eqS} (equivalent radii), respectively, along the length and the area of the middle turn, which were calculated using the formulas:

$$r_{eqL} = (r - w/2) + (a + b - 4r)/\pi, \tag{5}$$

$$r_{eqS} = \sqrt{((a - w)(b - w) + (\pi - 4)(r - w/2)^2)/\pi}. \tag{6}$$

As a result of the research, it was concluded that the use of spiral inductors made on a printed circuit board for both the transmitting and receiving modules was expedient, since this approach made it possible to achieve a high degree of reproducibility of the characteristics of the manufactured inductors. At the same time, the research was made of the turns' configuration influence on the active component of the inductors' impedance, which revealed a significant effect of the turns' proximity. Along with the surface effect, it adversely affected the active resistance of the inductors as the resonant frequency of the device increased [5].

In addition, it was necessary to determine the resonance circuit, which could be implemented for both current resonance and voltage resonance. The design of various circuits demonstrated the feasibility of using a series resonance circuit in both modules of the device.

Equivalent radius was calculated by the formula:

$$r_{eq} = r_{eqL} - \left(1 - \frac{w}{r_{eqL} + w}\right) (r_{eqL} - r_{eqS}). \quad (7)$$

The calculated inductance values were 50.2 μH and 36.3 μH for the transmitting and receiving inductors, respectively.

The next step was to calculate the values of the coupling coefficient of the inductors k :

$$k = \frac{M}{\sqrt{L_t L_r}}, \quad (8)$$

where M is the mutual inductance of coils, L_t и L_r is the inductance of transmitting and receiving inductors, respectively.

The mutual inductance between two flat coils can be calculated by replacing each of them with two turns, the radii of which are defined as $r_{avg} \pm w/8\sqrt{3}$, where r_{avg} was replaced by r_{eq} for rectangular inductors with rounded corners.

If the transmitting inductor is described by turns A and B , and the receiving one is described by C and D , then their mutual inductance can be described as

$$M \approx N_t N_r \frac{M_{AC} + M_{AD} + M_{BC} + M_{BD}}{4}, \quad (9)$$

where N_t и N_r are number of turns in one layer of inductors.

After calculating M using expressions (2) and (9), as well as the inductances of one layer of the coils (4) and placement of these values into (8), the distribution of k values was determined.

The calculation of the amplitude values of the current was made by the complex amplitudes' method. In general, the solution was reduced to a system of equations describing the equivalent circuit of the experimental facility:

$$\begin{cases} E_0 = i_1 \left(R_E + R_{L_t} + j\omega L_t + \frac{1}{j\omega C_t} \right) - i_2 \cdot j\omega M \\ i_1 \cdot j\omega M = i_2 \left(R_{L_r} + j\omega L_r + \frac{1}{j\omega C_r} + 2R_d + \frac{R_z R_{chg}}{R_z + R_{chg}} \right) \end{cases} \quad (10)$$

where ω is the operating frequency of the generator, E_0 and R_E are equivalent voltage and internal resistance of the generator's amplifier, i_1 and i_2 are currents in the transmitting and receiving circuits, R_{L_t} and R_{L_r} are the inductors' active resistance, C_t and C_r are the equivalent capacitance of resonant circuits calculated by the formula $C=1/(\omega^2 L)$, based on the resonant frequencies of the circuits of the experimental facility, R_d is the resistance of the diode of the rectifier bridge, R_z is the resistance of the Zener diode, R_{chg} is the resistance of the charge control module [6].

E_0 was calculated based on the idling parameters of the transmitting part:

$$E_0 = I_0 \sqrt{(R_E + R_{L_t})^2 + \left(\omega L_t - \frac{1}{\omega C_t}\right)^2}, \quad (11)$$

where I_0 is the no-load current in the transmitting inductor.

In the process of developing a methodology for assessing the impact of the energy fields of experimental prototypes of contactless charging of implant power sources on biological objects along with the calculation of the resistance of diodes, the effect of temperature conditions of inductors on the stability of tuning circuits to resonance was investigated (formula 12).

The resistance of the bridge diodes was expressed as

$$R_d(V) = V / \left(I_s \left(e^{\frac{qV}{nkT}} - 1 \right) \right), \tag{12}$$

where V is the diode voltage, $I_s=830 \cdot 10^{-9}$ is the reverse saturation current, $n=1$ is the emission coefficient, k is the Boltzmann constant, T is the temperature (K), q is the elementary electric charge.

4. Results of experimental assessing of the impact of the energy fields on biological objects

To increase the stability of further usage, capacitors of various form factors and from various dielectrics were tested. Among other things, the possibility of use of air trimmers, of lead-out ceramic capacitors' array for various installation technologies and different types of dielectrics was investigated. The question was relevant especially for the resonant circuit of the transmitting module due to its high quality and high amplitudes of its currents.

As a result, it was decided to abandon the use of air trimmers due to their high dimensions, cost, and low operational reliability in favor of SMT ceramic capacitors with a NP0 dielectric. Finally, various schemes for constructing the amplifier of the transmitter module of the device were tested using analytical, model, and full-scale methods [7, 8]. As a result, the D class amplifier circuit was chosen.

During the experiment, the voltage at the Zener diode did not exceed the threshold for its breakdown. It allowed us to describe its resistance as

$$R_z = V_r / I_r, \tag{13}$$

where $V_r=4$ V is the reverse voltage and $I_r=2$ μ A is the reverse current.

The permissible value of the charging current was limited by hardware. This value was not achieved at any mutual position of the inductors. This effect could be considered as an additional protection against the transition of the Zener diode into the breakdown mode.

The equivalent impedance of the integrated circuit (IC) of charge control was expressed as

$$R_{chg}(V, V_{bat}) = V / \left(\frac{V - V_{bat}}{R_{ds}} + I_s \right), \tag{14}$$

where V is the voltage at the input of the charge control IC, $V_{bat}=3.8$ V is the voltage across the battery, $R_{ds}=0.5$ Ω is the resistance of the field effect transistor built into the IC, $I_s=1.4$ mA is the own current consumption of the IC.

The theoretically achievable values of the output current of the receiving module of the charging device were calculated, the results of which are shown in figure 6 [9].

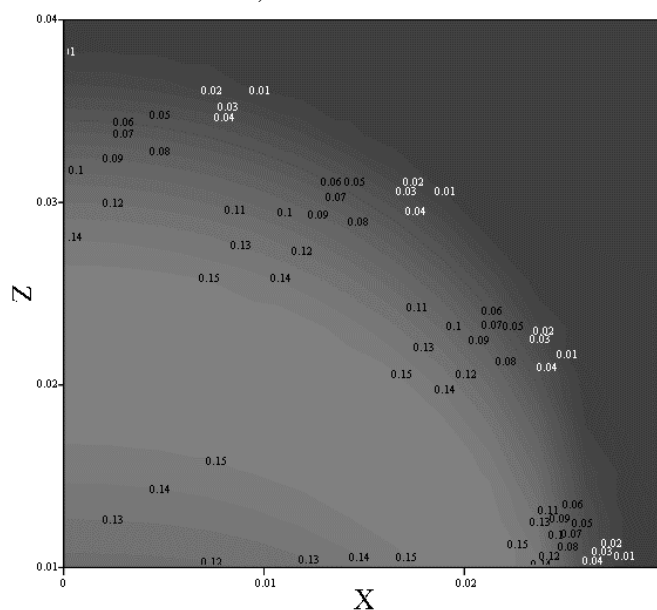


Figure 6. Distribution of output current [A] depending on the lateral (X) and axial displacement [m] of the antenna of the receiving module relative to the antenna of the transmitting module.

Preventing of short-term negative effects on biological tissues is reduced to controlling its temperature and preventing the maximum permissible level from being exceeded. Considering the variability of the distance between the transmitting and receiving modules of the device due to the mobility of the biological object, the device of wireless energy transfer provides automatic adjustment of the electromagnetic field power to ensure the safety of the biological object.

5. Conclusion

When implementing the methodology for assessing the impact of the energy fields of experimental prototype of implant power supplies' contactless charging on biological objects, it was decided to link the transmitting and receiving modules to negative feedback loop, which allows stabilizing the power supplied to the transmitting circuit by the D class amplifier. This solution minimizes the heating of the receiving module, both in the area of the receiving circuit, and in the area of the stabilizer of the charging current of the battery. Thus, in addition to smaller dimensions, the new solution allows optimizing the energy characteristics of the device as a whole.

Acknowledgment

The paper was prepared in the course of applied research "Development of an experimental prototype of device for wireless charging of implant batteries" (unique identifier of the project RFMEFI57817X0233) of the Federal target program "Research and development in priority areas of development of the scientific and technological complex of Russia for 2014-2020" of the Ministry of Science and Higher Education of the Russian Federation in the priority direction "Life Science".

References

- [1] Federal Law "On Amendments to Certain Legislative Acts of the Russian Federation on the Use of Information Technologies in the Field of Health Protection" No 242-FL July 29th, 2017
- [2] Ho J S, Yeh A J and Neofytou E 2014 Wireless power transfer to deep-tissue microimplants *Proc. Nat. Acad. Sci.* **111(22)** 7974–9
- [3] Wright P 2008 *Energy harvesting in the human body (Implantable self-powered sensors)* (New York: Emka PRESS) 215
- [4] Gorskii O V 2018 Potential power supply methods for implanted devices *Biomedical Engineering* **52(3)** 204-9
- [5] Gorskii O 2018 The role of impedance matching for depth adjustment of inductive charger for medical implants *Proceedings of the 23rd Conference of Open Innovations Association FRUCT* pp 135-42
- [6] Petrushevskaya A, Rabin A and Kilimnik V 2019 *Energy fields' impact on biological objects* (Proceedings of the 24th Conference of Open Innovations Association FRUCT) p 328-34
- [7] Singhal N, Nidhi N, Patel Rishi, Pamarti S 2011 A zero-voltage switching contour-based power amplifier with minimal efficiency degradation under back-off *IEEE Transactions on Microwave Theory and Techniques* **59(11)** 1589-98
- [8] Ozen M, Jos R, Andersson C M, Acar M and Fager C 2011 High efficiency RF pulse width modulation of class-E power amplifiers *IEEE Transactions on Microwave Theory and Techniques* **59(11)** 2931-42
- [9] Rabin A V, Merkova M A and Kilimnik V A 2019 Development of experimental prototype's module functional schemes for battery wireless recharging implants *Proceedings of the workshop "Advanced Technologies in Material Science, Mechanical and Automation Engineering", Krasnoyarsk*